



## Partial photocatalytic oxidation of glycerol in TiO<sub>2</sub> water suspensions

V. Augugliaro<sup>a,\*</sup>, H.A. Hamed El Nazer<sup>b</sup>, V. Loddo<sup>a</sup>, A. Mele<sup>c</sup>, G. Palmisano<sup>a,d</sup>, L. Palmisano<sup>a</sup>, S. Yurdakal<sup>a,e,f</sup>

<sup>a</sup> "Schiavello-Grillone" Photocatalysis Group, Dipartimento di Ingegneria Chimica dei Processi e dei Materiali, Università di Palermo, Viale delle Scienze, 90128 Palermo, Italy

<sup>b</sup> Photochemistry Department, National Research Centre, Al-Behos St. (El-Tahrir street), 12622 Dokki-Cairo, Egypt

<sup>c</sup> Dipartimento di Chimica, Materiali e Ingegneria Chimica G. Natta, Politecnico di Milano, Via L. Mancinelli 7, 20131 Milano, Italy

<sup>d</sup> Dipartimento di Ingegneria Elettronica, Università degli Studi di Roma "Tor Vergata", Via del Politecnico 1, 00133 Roma, Italy

<sup>e</sup> Kimya Bölümü, Fen Fakültesi, Anadolu Üniversitesi, Yunus Emre Kampüsü, 26470 Eskişehir, Turkey

<sup>f</sup> Kimya Bölümü, Fen-Edebiyat Fakültesi, Afyon Kocatepe Üniversitesi, Ahmet Necdet Sezer Kampüsü, 03100 Afyon, Turkey

### ARTICLE INFO

#### Article history:

Available online 18 February 2010

#### Keywords:

Glycerol partial oxidation  
Selective photocatalytic oxidation  
Titanium dioxide  
Reaction pathways

### ABSTRACT

The photo-oxidation of glycerol in aqueous suspensions containing commercial and home-prepared TiO<sub>2</sub> samples in the anatase, rutile or anatase–rutile polymorphic phases was investigated by using two different batch photoreactors, an annular photoreactor and a cylindrical photoreactor. The glycerol oxidation products detected in the aqueous phase were: 1,3-dihydroxyacetone, glyceraldehyde, formic acid and carbon dioxide. Two unknown compounds were also detected by electrospray ionization mass spectrometry as peaks at *m/z* 268 and *m/z* 176. A plausible mechanism for their formation was suggested based on ESI-MS and MS<sup>n</sup> experiments. The results indicate that in both systems the commercial samples showed the best performances both for reaction rate and selectivity toward 1,3-dihydroxyacetone, glyceraldehyde, formic acid and CO<sub>2</sub>.

© 2010 Elsevier B.V. All rights reserved.

### 1. Introduction

With an increase in environmental consciousness throughout the world, there is a challenge for chemists and chemical engineers to develop new products, processes and services that achieve necessary social, economical and environmental objectives. The Green Chemistry (environmentally benign chemistry) and Green Engineering areas, developed in these last years, are the answers of the scientific community to that challenge. As well as using and producing better chemicals with less waste, the challenge also involves reducing other associated environmental impacts including reduction in the amount of energy used in chemical processes [1–3].

The selective oxidation of alcohols is an important preparative method in organic chemistry. The resulting products, aldehydes and ketones [4–6], are extensively used as precursors and intermediates for the production of flavours, fragrances, and biologically active compounds. The application of these preparations, however, causes severe environmental problems due to waste from heavy metals or stoichiometric amounts of reagents and the generation of undesirable co-products [7–11]. From the standpoint of green and sustainable chemistry, there is still a need to develop cleaner catalytic oxidation systems.

Among alcohols, glycerol (1,2,3-propanetriol) has a widespread application; this molecule is used in toothpastes, pharmaceuticals, cosmetics, soaps and as sweetener in cakes and wetting agent in tobacco. Glycerol is now available in very huge amounts [12]; it is a co-product of oils and fats industries which have grown very much in last years. Moreover, nowadays glycerol is also obtained from biodiesel: one ton of biodiesel produces in fact about 100 kg of pure glycerol. Only small amounts of glycerol are used to synthesise other useful molecules as for instance polyethers and esters [12]. It is therefore of great concern to try to make value-added products from glycerol as an alternative to disposal by incineration. Consequently the researches aimed at the obtainment of functionalized glycerol in order to take advantage of its wide availability are up to date.

Many products can be obtained from glycerol partial oxidation: 1,3-dihydroxyacetone (DHA), glyceraldehyde (GAD), glyceric acid, glycolic acid, hydroxypyruvic acid, mesoxalic acid, oxalic acid, tartronic acid and all of them are considered chemicals for highly specialized applications. 1,3-Dihydroxyacetone is formed when the secondary hydroxyl group of glycerol is selectively oxidised and it is an important chemical used in the cosmetics industry as a tanning substance [13]. In addition to its main utilization in cosmetics, 1,3-dihydroxyacetone has also other applications, for instance as a monomer in polymeric biomaterials [12]. The oxidation of the primary hydroxyl groups of glycerol produces GAD, an intermediate of the carbohydrate metabolism.

\* Corresponding author. Tel.: +39 091 23863720; fax: +39 091 7025020.  
E-mail address: [augugliaro@dicpm.unipa.it](mailto:augugliaro@dicpm.unipa.it) (V. Augugliaro).

Glyceraldehyde is also a standard by which chiral molecules of the D- or L-series are compared.

Glycerol catalytic aerobic oxidation has been studied [12–20] by using Pd/C, Pt/C and more recently Au/C catalysts under different experimental conditions, and the distribution of the products and the selectivity were controlled by changing the temperature and the pH values of the reaction environment. For instance the oxidation in water over conventional precious metal based catalysts such as Au/C and Pt/C yielded glyceric acid [19,20]. It has been described also the oxidation of both primary hydroxyl groups of glycerol in the presence of Pt/CeO<sub>2</sub> catalysts that produced tartronic acid with a selectivity of 40% [21].

Electro-catalytic oxidation of glycerol mainly to DHA with tetramethyl piperidine-1-oxyl (TEMPO) as the oxidant agent and Ag/AgCl as the catalyst has been reported by Ciriminna et al. [13]. Only for long reaction times significant amount of hydroxyl-pyruvic acid was found.

Photocatalytic oxidation of some aromatic alcohols in water has been recently performed with high selectivity to the corresponding aldehydes, using home-prepared anatase, brookite or rutile TiO<sub>2</sub> [22–29].

As far as glycerol is concerned, Lichtin et al. [30] first reported its oxidative decomposition in liquid water by a TiO<sub>2</sub>-catalyzed photoprocess. As to concern the photocatalytic partial oxidation, up to date there is only one published work by Maurino et al. [31] reporting the photocatalytic selective oxidation of glycerol in water to DHA by using Degussa P25 and Merck TiO<sub>2</sub> catalysts and their fluorinated derivatives. By using fluorinated Degussa P25 and very low concentration of glycerol (ca. 1 mM), almost 100% selectivity to DHA was obtained for conversions lower than 30% and the intermediates were similar to the oxidation products in thermal catalysis.

In this work photocatalytic oxidation of glycerol was performed by using an annular and a cylindrical batch type photocatalytic reactor in the presence of commercial and home-made TiO<sub>2</sub> samples. The intermediates were determined and two of them (DHA and GAD) resulted the same of those obtained by thermal catalysis, while others were not found up to date both in thermal catalytic and photocatalytic studies.

## 2. Experimental

### 2.1. TiO<sub>2</sub> photocatalysts

Two commercial TiO<sub>2</sub> catalysts and two home-prepared TiO<sub>2</sub> powders were used for the photoreactivity runs. The commercial photocatalysts were: pure rutile TiO<sub>2</sub> (Sigma–Aldrich) and TiO<sub>2</sub> P25 (Degussa). TiO<sub>2</sub> P25 is a standard material in the field of photocatalytic reactions, it contains anatase and rutile phases in a ratio of about 4:1, the content of amorphous phase being very low (about 1.0%) [32]. In Table 1 some physico-chemical and morphological properties of these powders and two other justify home-prepared TiO<sub>2</sub> powders are reported.

#### 2.1.1. Home preparation of anatase TiO<sub>2</sub>

The preparation method has been reported elsewhere [23]. The precursor solution was obtained by adding 5 mL of TiCl<sub>4</sub> drop by

drop into a 200 mL beaker containing 50 mL of water. During the addition, that lasted 5 min, the solution was magnetically stirred by a cylindrical bar at 600 rpm. After that the beaker was closed and mixing was prolonged for 12 h at room temperature, eventually obtaining a clear solution. This solution was transferred into a round-bottom flask fitted with a graham condenser. The flask was heated in boiling water for 0.5 h, obtaining a white suspension at the end of each treatment. The suspensions were then dried at 323 K by means of a rotovapor machine (model Buchi Rotovapor M) working at 50 rpm, in order to obtain the final powdered catalysts. Hereafter the home-prepared anatase catalyst is referred to as HPA.

#### 2.1.2. Home preparation of rutile TiO<sub>2</sub>

The preparation method has been reported elsewhere [28]. The precursor solution was obtained by adding 20 mL of TiCl<sub>4</sub> to 1000 mL water contained in a volumetric flask; the addition was carried out very slowly in order to avoid warming of the sol as the TiCl<sub>4</sub> hydrolysis is a highly exothermic reaction. At the end the resulting sol was mixed for 2 min by a magnetic stirrer and then the flask was sealed and maintained at room temperature (ca. 298 K) for six days. The solid powder precipitated at the end of the whole treatment was separated by centrifugation (20 min at 5000 rpm) and dried at room temperature. The final home-prepared rutile catalyst is hereafter indicated as HPR.

### 2.2. Photocatalyst characterization

X-ray diffractometry (XRD) patterns of the powders were recorded by a Philips diffractometer (operating at a voltage of 40 kV and a current of 30 mA) using the CuK $\alpha$  radiation and a 2 $\theta$  scan rate of 1.28°/min. The crystalline sizes of the samples were determined by using the Scherrer equation [33,34].

Environmental scanning electron microscopy (ESEM) images were obtained using an ESEM microscope (Philips, XL30) operating at 25 kV. A thin layer of gold was evaporated on catalysts samples, previously sprayed on the stab and dried at room temperature. The sizes of secondary particles were determined by analyzing the images.

Brunauer–Emmett–Teller (BET) specific surface areas (SSA) were measured by the single-point BET method using a Micromeritics Flow Sorb 2300 apparatus. Before the measurement, the commercial samples were dried 1 h at 373 K, 2 h at 423 K and degassed 0.5 h at 423 K; on the contrary the home-prepared catalysts were only degassed at room temperature for 3 h. The tolerance of BET measurements was 4% and the SSA values for commercial specimens were almost the same of those furnished by producers.

### 2.3. Photoreactivity set up and procedure

The photocatalytic oxidation of glycerol in water was carried out by testing the TiO<sub>2</sub> samples (see Table 1) in the contemporaneous presence of light, dissolved oxygen and glycerol in the concentration range of 10–180 mM. Two different batch photoreactors, all made of Pyrex glass, were used: the first one was an annular photoreactor (APR, internal diameter, 72 mm; annulus

**Table 1**  
Crystalline phases (A, anatase; R, rutile), BET specific surface area (SSA), secondary particles and crystallites size of the TiO<sub>2</sub> samples.

Photocatalyst	Crystalline phases	SSA [m <sup>2</sup> /g]	Secondary particle size [nm]	Crystallite size [nm]
Sigma–Aldrich	R	2.5	240	52
Degussa P25	A(80%), R(20%)	50	80	30
HPR	R	118	719	6.8
HPA	A	235	28	5

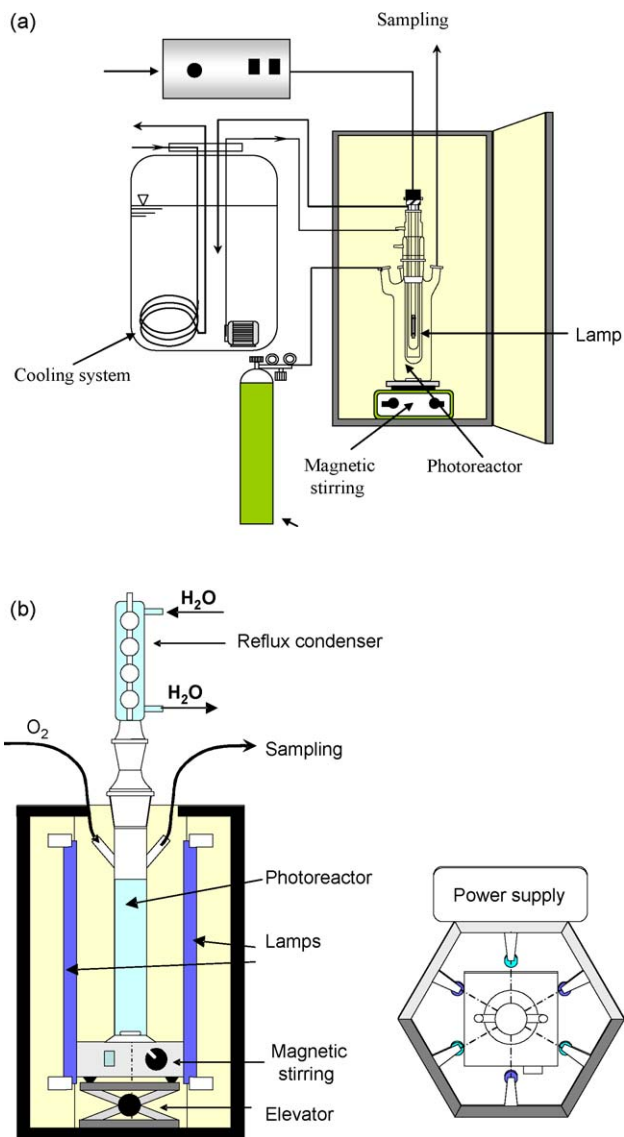


Fig. 1. Photoreactor schemes: (a) annular photoreactor and (b) cylindrical photoreactor.

gap, 20 mm) with immersed lamp (Fig. 1(a)) containing 0.5 L of aqueous suspension. It was provided with ports in its upper section for the inlet and outlet of oxygen and for sampling. A magnetic stirrer guaranteed a satisfactory suspension of the photocatalyst and the homogeneity of the reacting mixture. A 125 W medium pressure Hg lamp (Helios Italquartz, Italy) was axially positioned within the photoreactor; this non-coherent radiation source emits energy at the wavelengths of 313, 334, and mostly 366 nm. The lamp was cooled by water circulating through a Pyrex thimble; the temperature of the suspension was about 300 K. The radiation energy impinging on the suspension had an average value of  $10 \text{ mW/cm}^2$ . It was measured at 360 nm by using a radiometer UVX Digital.

The second photoreactor was a cylindrical photoreactor (CPR, internal diameter, 32 mm) (Fig. 1(b)), containing 220 mL of aqueous suspension. It was irradiated from the outside by means of six 15 W Philips fluorescent lamps whose main emission peak in the near-UV region is at 365 nm. In the course of the photocatalytic runs the temperature of the suspension was 318 K. A reflux condenser avoids loss of volatile organic molecules. With the six lamps turned on, the radiation energy impinging on the suspension

had an average value of  $1.2 \text{ mW/cm}^2$ . It was measured at 360 nm by using a radiometer UVX Digital.

Before switching on the lamp, oxygen was bubbled into the suspension for 30 min at room temperature to reach the thermodynamic equilibrium.

Samples of reacting suspension were withdrawn at fixed time intervals during the runs; they were immediately filtered through a  $0.45 \mu\text{m}$  hydrophilic membrane (HA, Millipore) before being analysed. The pH of the starting glycerol solution in the presence of the photocatalysts was adjusted to ca. 7. During the run pH values decrease due to production of formic acid.

#### 2.4. Analytical techniques

The quantitative determination and identification of glycerol and its oxidation products were performed by means of a Beckman Coulter HPLC (System Gold 126 Solvent Module and 168 Diode Array Detector), equipped with an Alltech IOA 1000 column. The analyses were performed at 192 nm. Standards of glycerol, GAD, DHA and formic acid (FA) were purchased from Sigma–Aldrich with a purity of  $>99\%$ . Retention times and UV spectra of the compounds were compared with those of standards. The eluent consisted of 0.005 M of  $\text{H}_2\text{SO}_4$ . Flow rate and analysis temperature were  $0.4 \text{ mL/min}$  and  $25^\circ\text{C}$ , respectively.

Total organic carbon analyses were carried out by using a 5000 A Shimadzu TOC analyser. Five measurements were performed for each sample the lowest and the highest values were rejected and the average value of the others was considered. Samples of initial concentrations equal to 10, 50, 100 and 180 mM were diluted 10, 50, 100 and 180 times, respectively.

Electrospray ionization mass spectrometry (ESI-MS) experiments were carried out on a Bruker Esquire 3000+ instrument with quadrupole ion trap detector (QITD). Stock solutions containing about  $1 \text{ mg/mL}$  of crude product were diluted 1:100 (v/v) in a mixture  $\text{H}_2\text{O/MeOH}$  (50:50 (v/v) both HPLC grade). The solutions thus prepared were analyzed by direct infusion in the ESI source at  $20 \mu\text{L min}^{-1}$ . Typical settings for MS acquisitions: needle voltage 4.5 kV, skimmer potential 40 V, end cap potential 250 V,  $\text{N}_2$  temperature  $280^\circ\text{C}$ , gas flow 11 L/min. Mass range was scanned from  $m/z$  50 to  $m/z$  500 at a rate of  $13,000 (m/z)/\text{s}$ .  $\text{MS}^2$  and  $\text{MS}^3$  experiments were carried out by isolation of precursor ion(s) in the quadrupole ion trap and collision with He gas.

### 3. Results and discussion

The used commercial photocatalysts showed to have lower specific surface areas (SSA) and higher crystallite sizes than the home-prepared ones (see Table 1). The secondary particles size of HPR sample showed to be the highest one, probably because the preparation method of this sample (with an aging time of six days) allowed the crystallites growth. XRD patterns of the used photo-

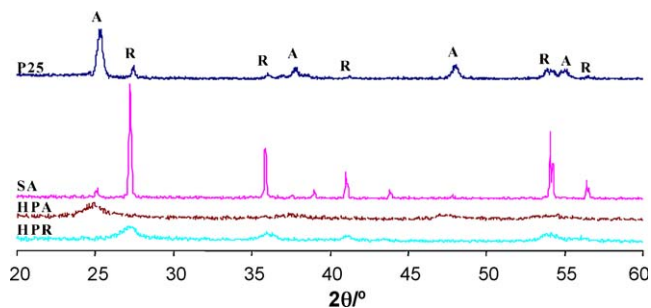


Fig. 2. XRD patterns of commercial and home-prepared  $\text{TiO}_2$  samples. P25, Degussa P25; SA, Sigma–Aldrich Rutile; HPA, home-prepared anatase; HPR, home-prepared rutile.

**Table 2**

Results of photocatalytic oxidation of glycerol obtained by using APR reactor. Used catalyst, catalyst amount, glycerol initial concentration, irradiance measured at the external wall of reactor, reaction time required for 35% conversion ( $t_{35\%}$ ) and selectivities ( $S$ ) towards the known products.

Catalyst	Catalyst amount [g/L]	Glycerol [mM]	Leaving irradiance [mW/cm <sup>2</sup> ]	$t_{35\%}$ [h]	$S_{\text{GAD}}$ [%]	$S_{\text{DHA}}$ [%]	$S_{\text{FA}}$ [%]	$S_{\text{CO}}$ [%]
Homogeneous	–	100	–	17 <sup>a</sup>	4.5 <sup>a</sup>	3.7 <sup>a</sup>	6.5 <sup>a</sup>	
Degussa P25	0.1	100	0.8	24.5	7	4	3	17.4
Degussa P25	0.2	100	0.15	21	5.7	4	4.2	20.3
Degussa P25	0.4	100	0.02	70	11	8	4.8	11.5
Degussa P25	0.2	10	0.02	6.5	10	6.5	3.1	12.5
Degussa P25	0.1	175	0.8	28	9	5	7	16
Degussa P25	0.1	53	0.8	14.5	9	5.5	4	17.4
Sigma–Aldrich	0.2	100	2.63	20	5.5	3	5	12.6
Sigma–Aldrich	0.4	100	0.8	31	10.5	5.2	10	23.7
Sigma–Aldrich	0.4	10	0.8	8.5	8	5	6.1	18.5
HPR	0.2	100	0.8	30	4	2.5	3.7	11.1
HPR	0.4	100	0.02	40	4	2.9	2.2	10.9
HPR	0.4	10	0.02	6	1.8	2.2	4	13.8
HPA	0.3	100	0.8	32	6.5	5	7.4	21.1

<sup>a</sup> Data obtained for 5% conversion.

catalysts are provided in Fig. 2. The main peaks of anatase and rutile phases can be easily recognized [23,28]. It can be however noticed that the peaks of HP samples diffractograms are much broader than the others. This is mainly due to the absence of a thermal treatment in their preparation (see Section 2), so that HP samples are nanostructured and less crystalline with respect to the commercial ones.

The contemporary presence of irradiation, catalyst and dissolved oxygen was needed for observing a significant oxidation of glycerol. The photoreactivity runs carried out in the absence of catalyst by using the APR photoreactor gave rise to a low glycerol conversion, only 5% mol after 17 h illumination. The homogeneous conversion in the CPR photoreactor was also quite low: 12.8 h of illumination were needed for reaching 5% mol conversion. Consequently the homogeneous process was not considered throughout this work because it was negligible with respect to the heterogeneous one.

The glycerol oxidation products detected in the liquid phase were: 1,3-dihydroxyacetone, glyceraldehyde, formic acid and carbon dioxide. Two unknown compounds were also detected by ESI-MS as peaks at  $m/z$  176 (hereafter indicated as “Product A”) and  $m/z$  268 (hereafter indicated as “Product B”).

The process performance was followed by measuring the values of glycerol, DHA, GAD and FA concentrations and calculating the substrate conversion and the product selectivities, i.e., the ratio between the produced moles of DHA, GAD or FA and the moles of converted glycerol. CO<sub>2</sub> concentration during the reaction was determined by subtracting the total organic carbon (TOC) concentration, experimentally determined at a certain time, from the initial concentration of organic carbon (entirely deriving from glycerol). As formic acid and carbon dioxide only contain one C atom, FA and CO<sub>2</sub> selectivities were calculated dividing by three their concentrations in order to have a correct comparison.

### 3.1. Photocatalytic reactivity in APR and CPR reactors

Table 2 reports the results of glycerol photocatalytic oxidation performed by using the APR reactor. It can be noticed that glycerol reacted in homogeneous conditions under irradiation even though with a very low reaction rate. The commercial samples showed the best performances both for reaction rate and products selectivity. The experiments carried out in order to study the influence of photocatalyst amount both on reaction rate and selectivity indicated that they do not appreciably change for Degussa P25 by increasing the amount from 0.1 to 0.2 g/L, whereas reaction rate enormously decreased (see  $t_{35\%}$  column in Table 2) and selectivity increased in the presence of 0.4 g/L. As far as Sigma–Aldrich (SA) is

concerned, the reaction rate decreased by increasing the photocatalyst amount from 0.2 to 0.4 g/L, remaining significantly higher with respect to P25, but the selectivity increased. Selectivities towards GAD were quite similar to those of P25, whereas selectivities towards DHA and FA were higher for P25 and SA, respectively. The best selective sample between HPR and HPA was the latter one, although these selectivity values towards GAD and DHA were lower than that obtained in the presence of the commercial samples. The results obtained by using Degussa P25 showed a higher accumulation of products when the leaving irradiance (i.e., the irradiance measured at the external wall of reactor) was lower than ca. 1% of the incident one, differently from the experiments carried out with values equal to ca. 8%. This could be due to an unsatisfactory irradiation of a fraction of the photocatalyst (present in excess when the transmitted light was very low). For Degussa P25 an amount of 0.1 g/L appeared to be the best compromise between reaction rate and selectivity.

The global selectivity to GAD, DHA, FA and CO<sub>2</sub> had an average value of ca. 35% mol with respect to the converted glycerol. HPLC analyses indicated the presence of other compounds (named Product A and Product B, with  $m/z$  176 and  $m/z$  268, respectively, as showed in ESI-MS results reported in the following).

At the end of each run the carbon contained in the remaining glycerol and in the produced GAD, DHA, FA and CO<sub>2</sub> was calculated. As expected, the balance was not satisfactory because in the absence of commercial standards it was not possible to determine the amounts of Product A and Product B.

It is important to report that, even for long lasting runs, the catalyst powder did not show any modification and activity loss throughout the experiments.

Table 3 reports the results of glycerol photo-oxidation performed by using CPR reactor. Under the used experimental conditions, both reaction rate and selectivity increased for all the samples, due to the different reactor geometries and irradiation fields. It can be noticed that this system seemed globally more efficient than APR reactor. Indeed, the times required for a conversion of 35% are lower and the selectivities towards the products are higher than those obtained by using the APR reactor. The best performances were obtained by using 0.091 g/L of Degussa P25 with an incident photon flow equal to 0.6 mW/cm<sup>2</sup>.

The global selectivity to GAD, DHA, FA and CO<sub>2</sub> had an average value of ca. 45% mol with respect to the reacted glycerol. HPLC analyses, moreover, again indicated the presence of Product A and Product B previously mentioned (with  $m/z$  176 and  $m/z$  268, respectively, as showed in ESI-MS results in the following).

Fig. 3 shows the data of a representative run carried out in the presence of Degussa P25 by using the APR reactor. The

**Table 3**

Results of photocatalytic oxidation of glycerol obtained by using CPR reactor. Used catalyst, catalyst amount, glycerol initial concentration, reaction time required for 35% conversion ( $t_{35\%}$ ) and selectivities ( $S$ ) towards the known products.

Catalyst	Catalyst amount [g/L]	Glycerol [mM]	$t_{35\%}$ [h]	$S_{GAD}$ [%]	$S_{DHA}$ [%]	$S_{FA}$ [%]	$S_{CO_2}$ [%]
Homogeneous	–	100	12.8 <sup>a</sup>	13 <sup>a</sup>	7.2 <sup>a</sup>	7 <sup>a</sup>	
Degussa P25	0.023	100	12	13	7.5	8	20.3
Degussa P25	0.046	100	12	8	6.2	6.3	29.1
Degussa P25	0.091	100	10	10	7	8.8	26.6
Degussa P25	0.182	100	13	8	7	6.8	31.2
Degussa P25	0.364	100	13	7	7	4	37.7
Degussa P25 <sup>b</sup>	0.091	100	14.5	13	8	8	11.7
Degussa P25	0.091	185	12	11	6.3	14	14.3
Degussa P25	0.091	55	5.2	12	7.5	6.5	20.6
Sigma–Aldrich	0.091	100	7.7	9.5	4.5	8	7.1
HPR	0.091	100	11	6.5	4.6	5.5	29.4
HPA	0.091	100	18	6.9	5.4	6.9	18.3

<sup>a</sup> Data obtained for 5% conversion.

<sup>b</sup> Data obtained by using an incident photon flux of 0.6 mW/cm<sup>2</sup>.

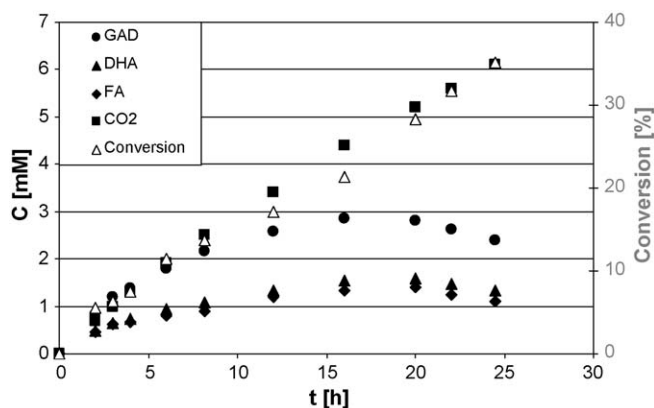


**Fig. 3.** Concentration of 1,3-dihydroxyacetone, glyceraldehyde, formic acid and carbon dioxide and conversion for a run carried out with the APR reactor. Glycerol initial concentration, 100 mM. Photocatalyst: Degussa P25 (0.1 g/L). FA and CO<sub>2</sub> concentrations were divided by three for comparison aim.

concentrations of GAD, DHA, CO<sub>2</sub> (divided by three for the sake of comparison) and FA (divided by three for the sake of comparison) are represented along with the conversion values in the course of irradiation. Fig. 4 shows analogous results obtained with the CPR reactor.

In both cases the evolution of the oxidation products occurred simultaneously, indicating that parallel reactions are responsible for their production.

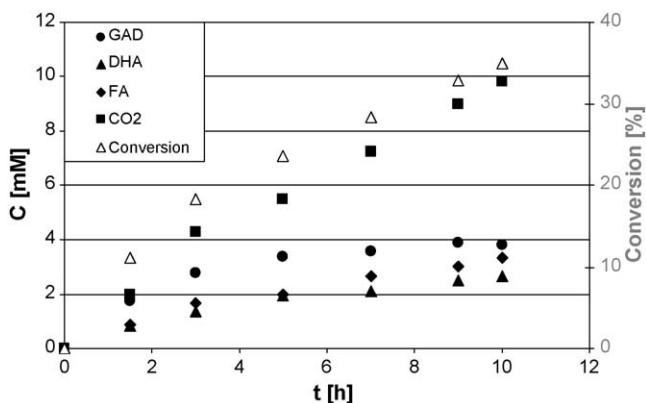


**Fig. 4.** Concentration of 1,3-dihydroxyacetone, glyceraldehyde, formic acid and carbon dioxide and conversion for a run carried out with the CPR reactor. Glycerol initial concentration, 100 mM. Photocatalyst: Degussa P25 (0.1 g/L). FA and CO<sub>2</sub> concentrations were divided by three for comparison aim.

It is worth noting that Degussa P25 showed to be more selective towards GAD, DHA and FA formation, in contrast with other photoreactions involving aromatic alcohols yielding higher selectivities in the presence of less crystalline home-prepared TiO<sub>2</sub> samples [22–29]. In the glycerol structure, indeed, differently from aromatic alcohols, three hydroxyl groups are present and consequently adsorption and desorption of reagents and products, respectively, occur in different extents and with different strengths [35,36].

Moreover it is very likely that Product A with  $m/z$  176 derives from two molecules of glyceric acid adsorbed onto the surface. This hypothesis is in accord also with a preliminary investigation by Amadelli [37] which found that glyceric acid is more strongly adsorbed onto TiO<sub>2</sub> surface than both glycerol and GAD. These findings indicate that the selectivity depends not only on photocatalyst samples, but also on substrate specificity and oxidation products.

The results showed in Fig. 3 indicate that the products concentration increased up to 15–20 h of reaction, then started to decrease demonstrating a subsequent over-oxidation, whereas the data obtained by using CPR reactor (Fig. 4) show a continuous increase of the products concentration that reached a plateau for times higher than 10 h.

From the analyses of the results, it may be hypothesized that the catalyst surface is not specialized to perform only one reaction but, on the contrary, that it is a highly heterogeneous one with the presence of different active sites that generate different products.

### 3.2. ESI-MS results

ESI-MS analyses were performed on samples withdrawn from both systems and showed the same results.

The full scan spectrum of the reaction mixture showed the presence of several peaks, mostly assigned by comparison with analytical standards. Along with glycerol, the main component of the blend, DHA and GAD were identified as peaks at  $m/z$  145. Sequential enrichment of the solution with DHA and GAD allowed us to unambiguously assign the peak at  $m/z$  145 as [DHA + MeOH + Na]<sup>+</sup> and [GAD + MeOH + Na]<sup>+</sup> adducts.

The mass spectrum of the reaction mixture showed also two unknown products at  $m/z$  177 and  $m/z$  269. The values of 176 and 268 correspond to the molecular weight of the unknown compounds A and B. The ESI ionization source converts these neutral molecules into positively charged ions detected at  $m/z$  177 and  $m/z$  269, respectively, by attachment of H<sup>+</sup> during the electrospray ionization process. This is the reason why the peaks related to unknown A and B are reported as  $m/z$  177 and  $m/z$  269 rather than 176 and 268. The structure of the corresponding ions

**Table 4**  
Summary of MS<sup>2</sup> experiments.

Precursor ion <i>m/z</i>	Fragment ion <i>m/z</i> and relative intensity
269	223 (47)
	195 (4)
	177 (100)
	131 (3)
177	149 (17)
	131 (100)

was investigated by MS<sup>2</sup> and MS<sup>3</sup> experiments. In both cases the collision potential was calibrated in such a way to retain 10% of the isolated precursor ion intensity. The results of the MS<sup>2</sup> experiments are summarized in Table 4.

These fragmentations deserve further comments. The fragment ion at *m/z* 223 comes from the precursor by neutral loss of 46 Da, consistent with formic acid release. This fact is consistent with the presence of a carboxy functional group in the structure of the precursor. The base peak at *m/z* 177 can be seen as deriving from the parent ion by neutral loss of the elements of glycerol (92 Da), suggesting that the structure of the precursor ion could be thought as the addition product of glycerol to a possible oxidation product

of glycerol itself. This working hypothesis is also substantiated by MS<sup>3</sup> experiments carried out on the fragment at *m/z* 223. The results are displayed in Fig. 5. Isolation and fragmentation of *m/z* 223 leads, as the only collision induced fragment, to the ion at *m/z* 131 via 92 Da neutral loss.

Combining these two experimental findings, we can confidently consider the carboxy functional group and the entire molecule of glycerol as building blocks of the unknown product whose protonated form gives rise to the peak at *m/z* 269. Additionally, the neutral loss of 28 Da observed on passing from *m/z* 223 to *m/z* 195 in the MS<sup>2</sup> experiment suggests the presence of a keto functional group in the precursor ion. At this stage a reasonable structure for *m/z* 269 and a consistent fragmentation pathway can be postulated. The scheme is sketched in Fig. 6. In this figure the large fragment is reported as protonated adduct of a compound of molecular weight 268 Da. It is therefore reported as *m/z* 269. As we are not able to locate the protonation site (e.g., H<sup>+</sup> may be attached to one of the two carbonyl groups or to any OH group) H<sup>+</sup> is generically indicated at the top of the molecular formula corresponding to the putative structure of the fragment at *m/z* 269.

The second unknown product detected in the mixture as the peak at *m/z* 177 is structurally related to the product discussed above. Indeed, both unknown products share the fragment at *m/z*

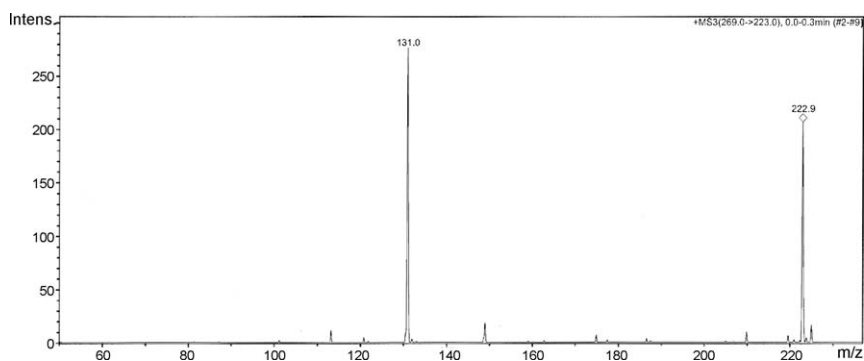


Fig. 5. MS<sup>3</sup> experiment corresponding to 269 → 223 → fragmentation.

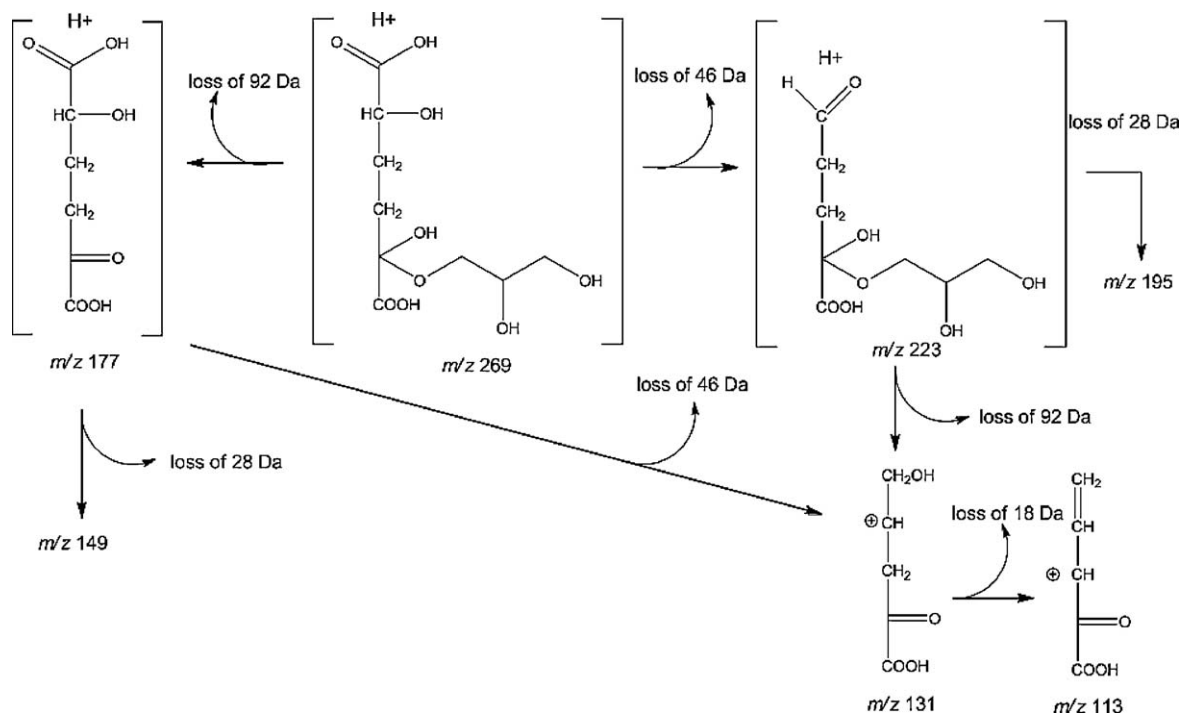
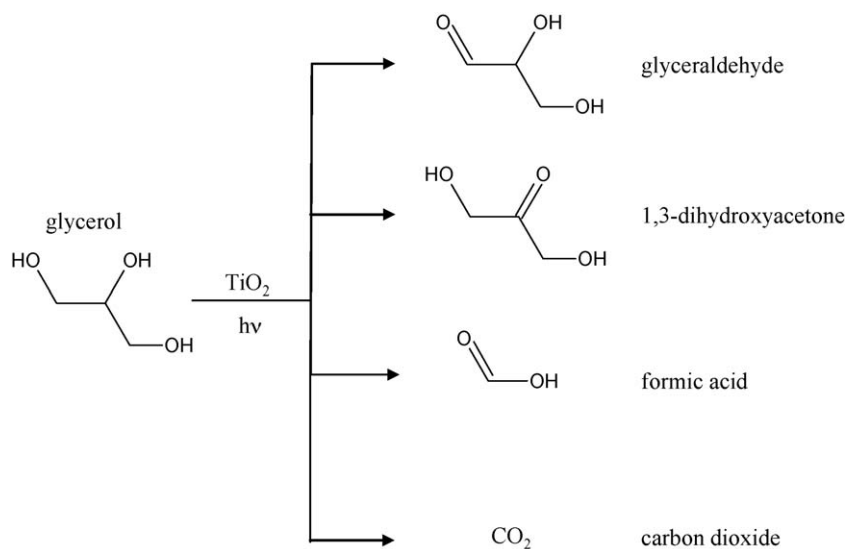
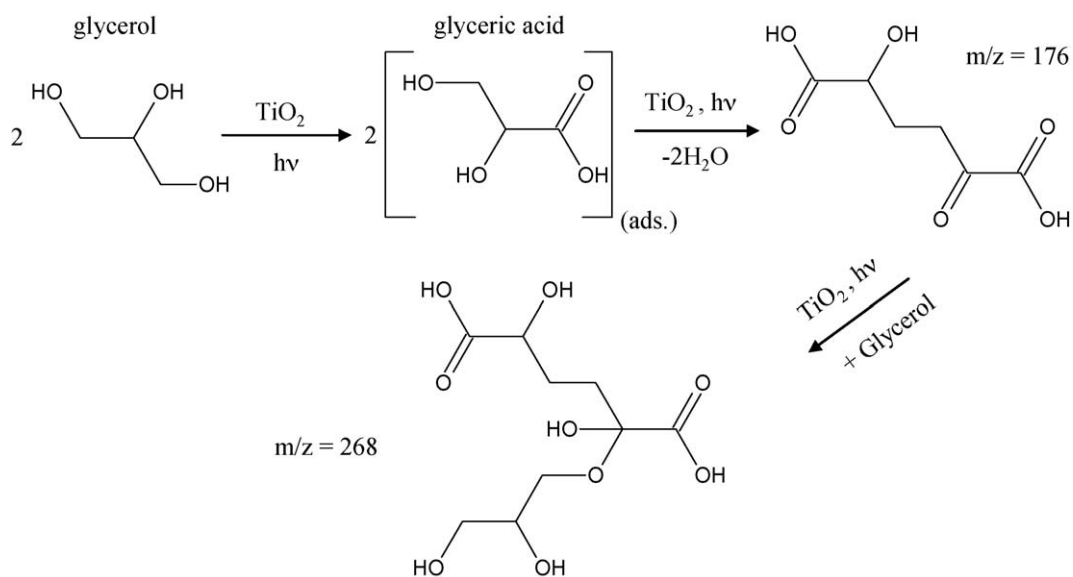


Fig. 6. Sketch of putative structures and fragmentation pathways from MS<sup>2</sup> experiments on *m/z* 269 and *m/z* 177.



Scheme 1.



Scheme 2.

131 and, as a matter of fact, the second product is also a fragment of the first one. MS<sup>3</sup> experiment on *m/z* 131 gave, as only fragment, *m/z* 113, consistent with the presence of a primary OH functionality in the precursor, as sketched in Fig. 6.

According to HPLC and ESI-MS analyses, Schemes 1 and 2 for products formation can be presented:

Scheme 1 shows the hypothesised reaction pathways in which GAD, DHA, FA and CO<sub>2</sub> are contemporaneously produced, whereas Scheme 2 indicates a likely pathway for the formation of Product A (*m/z* 176 compound) from glyceric acid molecules strongly adsorbed on the photocatalytic surface. This compound can subsequently react with a glycerol molecule giving rise to Product B (*m/z* 268 compound).

The absence of a second keto-group in the molecule *m/z* 176 could be due to its desorption before another subsequent surface oxidation. In fact the interaction of a CO group with the surface hydroxyls is weaker than that of OH alcoholic group.

#### 4. Conclusions

The partial photocatalytic oxidation of glycerol was performed by using two different systems in the presence of commercial and home-prepared TiO<sub>2</sub> samples in the anatase, rutile or anatase–rutile polymorphic phases. Contrarily to the results present in the literature for the photo-oxidation of some aromatic alcohols to the corresponding aldehydes, generally the most crystalline TiO<sub>2</sub> commercial samples showed the best performances both for reaction rates and products selectivities. Probably, the presence of three OH groups in glycerol and the different experimental conditions used determined this different behaviour. Moreover the high heterogeneity of surface and the likely presence of different active sites resulted in the formation of different products with relatively low selectivities. Products with molecular weights higher than that of glycerol were found as peaks at *m/z* 176 and *m/z* 268 of ESI-MS spectra.

## References

- [1] M. Kidwai, R. Mohan, Green chemistry: an innovative technology, *Found. Chem.* 7 (2005) 269–287.
- [2] J.C. Warner, A.S. Cannon, K.M. Dye, Green chemistry, *Environ. Impact Assess. Rev.* 24 (2004) 775–799.
- [3] M.M. Kirchhoff, Promoting sustainability through green chemistry, *Res. Conserv. Recycl.* 44 (2005) 237–243.
- [4] C.Y. Lorber, I. Pauls, J.A. Osborn, Catalyzed oxidation of alcohols by cis-dioxomolybdenum(VI) complexes via oxygen atom transfer from sulfoxide, *Bull. Soc. Chim. Fr.* 133 (1996) 755–758.
- [5] K.S. Coleman, L.J.L. Bedel, J.A. Osborn, Catalytic oxidation of alcohols to aldehydes or ketones using osmium-oxo complexes with sulfoxides or N-methylmorpholine-N-oxide as the co-oxidant: a comparative study, *C. R. Acad. Sci. Ser. IIc: Chem.* 3 (2000) 765–769.
- [6] Y. Kurusu, An oxidation system for green chemistry: the oxidation of alcohols and hydrocarbons in the presence of metal-polymer complexes, *J. Inorg. Organomet. Polym. Mater.* 10 (2000) 127–144.
- [7] G. ten Brink, I.W.C.E. Arends, R.A. Sheldon, Green, catalytic oxidation of alcohols in water, *Science* 287 (2000) 1636–1639.
- [8] R.A. Sheldon, I.W.C.E. Arends, G. ten Brink, A. Dijkstra, Green, catalytic oxidations of alcohols, *Acc. Chem. Res.* 35 (2002) 774–781.
- [9] D.I. Enache, J.K. Edwards, P. Landon, B. Solsona-Espriu, A.F. Carley, A.A. Herzing, M. Watanabe, C.J. Kiely, D.W. Knight, G.J. Hutchings, Solvent-free oxidation of primary alcohols to aldehydes using Au-Pd/TiO<sub>2</sub> catalyst, *Science* 311 (2006) 362–365.
- [10] C. Li, L. Chen, Organic chemistry in water, *Chem. Soc. Rev.* 35 (2006) 68–82.
- [11] K. Ohkubo, K. Suga, S. Fukuzumi, Solvent-free selective photocatalytic oxidation of benzyl alcohol to benzaldehyde by molecular oxygen using 9-phenyl-10-methylacridinium, *Chem. Commun.* 19 (2006) 2018–2020.
- [12] A. Behr, J. Eilting, K. Irawadi, J. Leschinski, F. Lindner, Improved utilisation of renewable resources: new important derivatives of glycerol, *Green Chem.* 10 (2008) 13–30.
- [13] R. Ciriminna, G. Palmisano, C. Della Pina, M. Rossi, M. Pagliaro, One-pot electrocatalytic oxidation of glycerol to DHA, *Tetrahedron Lett.* 47 (2006) 6993–6995.
- [14] C.L. Bianchi, P. Canton, N. Dimitratos, F. Porta, L. Prati, Selective oxidation of glycerol with oxygen using mono and bimetallic catalysts based on Au, Pd and Pt metals, *Catal. Today* 102–103 (2005) 203–212.
- [15] S. Demirel-Gülen, M. Lucas, P. Claus, Liquid phase oxidation of glycerol over carbon supported gold catalysts, *Catal. Today* 102–103 (2005) 166–172.
- [16] P. Gallezot, Selective oxidation with air on metal catalysts, *Catal. Today* 37 (1997) 405–418.
- [17] S. Carrettin, P. McMorn, P. Johnston, K. Griffin, G.J. Hutchings, Selective oxidation of glycerol to glyceric acid using a gold catalyst in aqueous sodium hydroxide, *Chem. Commun.* (2002) 696–697.
- [18] S. Demirel, K. Lehnert, M. Lucas, P. Claus, Use of renewables for the production of chemicals: glycerol oxidation over carbon supported gold catalysts, *Appl. Catal. B: Environ.* 70 (2007) 637–643.
- [19] R. Garcia, M. Besson, P. Gallezot, Chemoselective catalytic oxidation of glycerol with air on platinum metals, *Appl. Catal. A: Gen.* 127 (1995) 165–176.
- [20] N. Dimitratos, J.A. Lopez-Sanchez, D. Lennon, F. Porta, L. Prati, Effect of particle size on monometallic and bimetallic (Au,Pd)/C on the liquid phase oxidation of glycerol, *Catal. Lett.* 108 (2006) 147–153.
- [21] P. Fordham, M. Besson, P. Gallezot, Selective catalytic oxidation of glyceric acid to tartronic and hydroxypyruvic acids, *Appl. Catal. A: Gen.* 133 (1995) L179–L184.
- [22] V. Loddo, S. Yurdakal, G. Palmisano, G.E. Imoberdorf, H.A. Irazoqui, O.M. Alfano, V. Augugliaro, H. Berber, L. Palmisano, Selective photocatalytic oxidation of 4-methoxybenzyl alcohol to p-anisaldehyde in organic-free water in a continuous annular fixed bed reactor, *Ind. J. Chem. React. Eng.* 5 (2007) A57.
- [23] G. Palmisano, S. Yurdakal, V. Augugliaro, V. Loddo, L. Palmisano, Photocatalytic selective oxidation of 4-methoxybenzyl alcohol to aldehyde in aqueous suspension of home-prepared TiO<sub>2</sub> catalyst, *Adv. Synth. Catal.* 349 (2007) 964–970.
- [24] S. Yurdakal, G. Palmisano, V. Loddo, V. Augugliaro, L. Palmisano, Nanostructured rutile TiO<sub>2</sub> for selective photocatalytic oxidation of aromatic alcohols to aldehydes in water, *J. Am. Chem. Soc.* 130 (2008) 1568–1569.
- [25] V. Augugliaro, T. Caronna, V. Loddo, G. Marci, G. Palmisano, L. Palmisano, S. Yurdakal, Oxidation of aromatic alcohols in commercial and home-prepared irradiated rutile TiO<sub>2</sub> aqueous suspensions: a selectivity study, *Chem. Eur. J.* 14 (2008) 4640–4646.
- [26] V. Augugliaro, H. Kisch, V. Loddo, M.J. López-Muñoz, C. Márquez-Álvarez, G. Palmisano, L. Palmisano, F. Parrino, S. Yurdakal, Photocatalytic oxidation of aromatic alcohols to aldehydes in aqueous suspension of home-prepared titanium dioxide. 1. Selectivity enhancement by aliphatic alcohols, *Appl. Catal. A* 349 (2008) 182–188.
- [27] M. Addamo, V. Augugliaro, M. Bellardita, A. Di Paola, V. Loddo, G. Palmisano, L. Palmisano, S. Yurdakal, Environmentally friendly photocatalytic oxidation of aromatic alcohol to aldehyde in aqueous suspension of brookite TiO<sub>2</sub>, *Catal. Lett.* 126 (2008) 58–62.
- [28] S. Yurdakal, G. Palmisano, V. Loddo, O. Alagöz, V. Augugliaro, L. Palmisano, Selective photocatalytic oxidation of 4-substituted aromatic alcohols in water with rutile TiO<sub>2</sub> prepared at room temperature, *Green Chem.* 11 (2009) 510–516.
- [29] V. Augugliaro, V. Loddo, M. López-Muñoz, C. Márquez-Álvarez, G. Palmisano, L. Palmisano, S. Yurdakal, Home-prepared anatase, rutile, and brookite TiO<sub>2</sub> for selective photocatalytic oxidation of 4-methoxybenzyl alcohol in water: reactivity and ATR-FTIR study, *Photochem. Photobiol. Sci.* 8 (2009) 663–669.
- [30] N.N. Lichtin, J. Dong, K.M. Vijayakumar, Photopromoted TiO<sub>2</sub>-catalyzed oxidative decomposition of organic pollutants in water and in the vapor phase, *Water Pollut. Res. J. Can.* 27 (1992) 203–210.
- [31] V. Maurino, A. Bedini, M. Minella, F. Rubertelli, E. Pelizzetti, C. Minero, Glycerol transformation through photocatalysis: a possible route to value-added chemicals, *J. Adv. Ox. Technol.* 11 (2008) 184–192.
- [32] T. Ohno, K. Sarukawa, K. Tokieda, M. Matsumura, Morphology of a TiO<sub>2</sub> photocatalyst (Degussa, P-25) consisting of anatase and rutile crystalline phases, *J. Catal.* 203 (2001) 82–86.
- [33] P. Scherrer, Estimation of the size and internal structure of colloidal particles by means of roentgen, *Nachr. Ges. Wiss. Göttingen, Math.-Phys. Kl.* 2 (1918) 96–100.
- [34] A.W. Burton, K. Ong, T. Rea, I.Y. Chan, On the estimation of average crystallite size of zeolites from the Scherrer equation: a critical evaluation of its application to zeolites with one-dimensional pore systems, *Micropor. Mesopor. Mater.* 117 (2009) 75–90.
- [35] V. Augugliaro, H. Kisch, V. Loddo, M.J. López-Muñoz, C. Márquez-Álvarez, G. Palmisano, L. Palmisano, F. Parrino, S. Yurdakal, Photocatalytic oxidation of aromatic alcohols to aldehydes in aqueous suspension of home prepared titanium dioxide. 2. Intrinsic and surface features of catalysts, *Appl. Catal. A: Gen.* 349 (2008) 189–197.
- [36] A. Da Pozzo, M. Mascia, S. Palmas, A.M. Polcaro, J. Rodriguez Ruiz, A. Vacca, Innovative processes for oxidation of glycerol aqueous solutions, *Electrochem* 09, Manchester, UK, September 2009.
- [37] R. Amadelli, Private communication.